CHAPTER 4

Results and Discussion

4.1 UV/Vis spectrophotometer Results

The optical constant of the prepared samples have been to calculated from results that collected from UV/Vis spectrophotometer in the wavelength range (288 – 500) nm show that all fig com :-

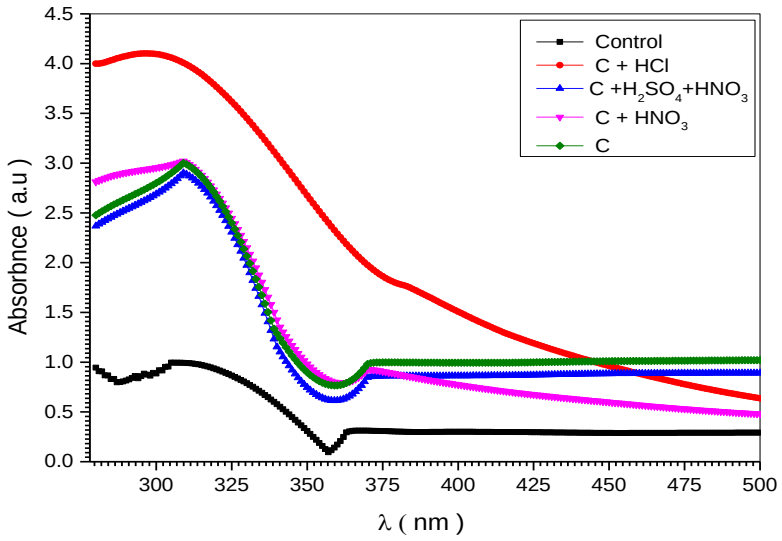

Fig (4.1.1) The optical absorbance spectra of Wooden Carbon Sinag treated by three acids (HCL, HNO3 and H_2SO_4:HNO_3 mixture) and one is untreated compared with control Multi Wall Carbon Nanotube sample (MWCNT).

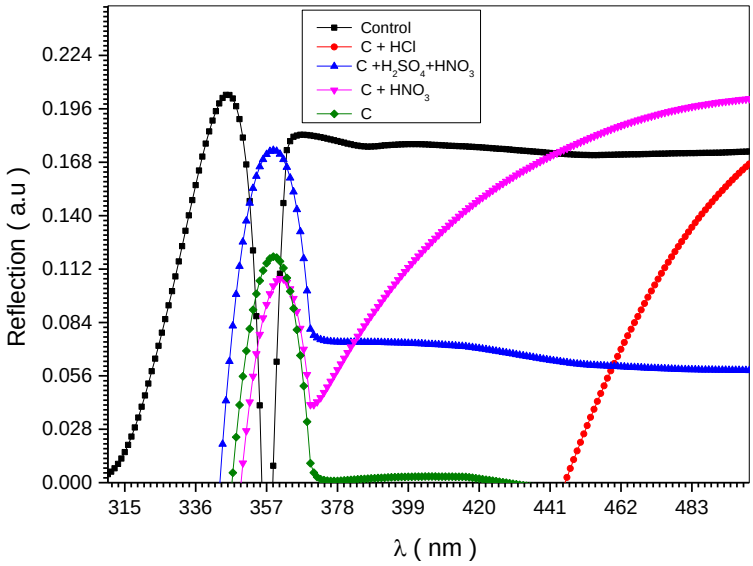

Fig (4.1.2) the reflectance spectra of Wooden Carbon Sinag treated by three acids (HCL, HNO_3 and H_2SO_4:HNO_3 mixture) and one is untreated compared with control Multi Wall Carbon Nanotube sample (MWCNT).

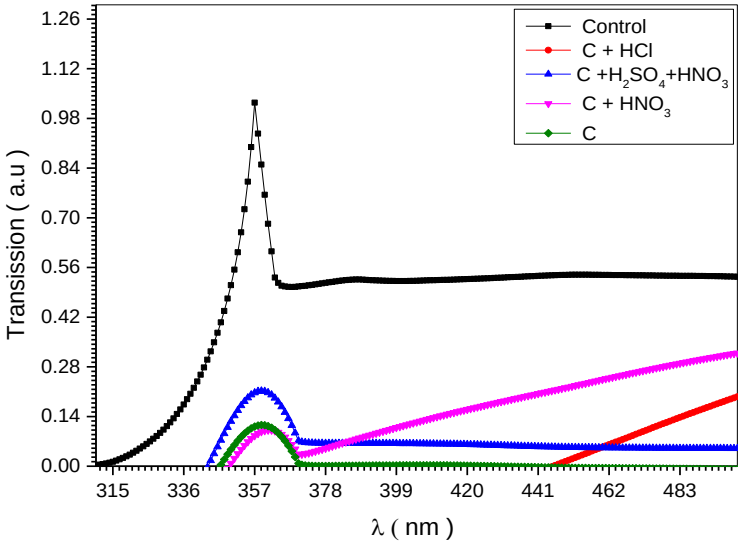

Fig (4.1.3) the transmission spectra of Wooden Carbon Sinag treated by three acids (HCL, HNO_3 and H_2SO_4:HNO_3 mixture) and one is untreated compared with control Multi Wall Carbon Nanotube sample (MWCNT).

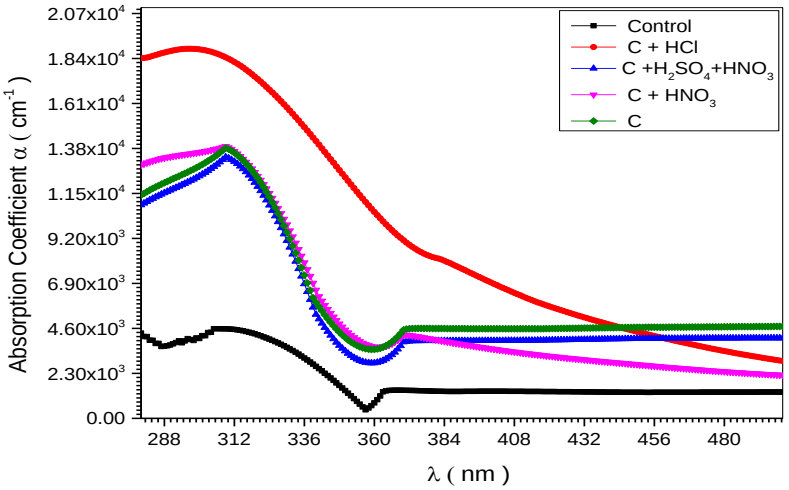

Fig (4.1.4) The variation absorption coefficient (α) with wavelength for Wooden Carbon Sinag treated by three acids (HCL,HNO_3 and H_2SO_4:HNO_3 mixture) and one is untreated compared with control Multi Wall Carbon Nanotube sample (MWCNT).

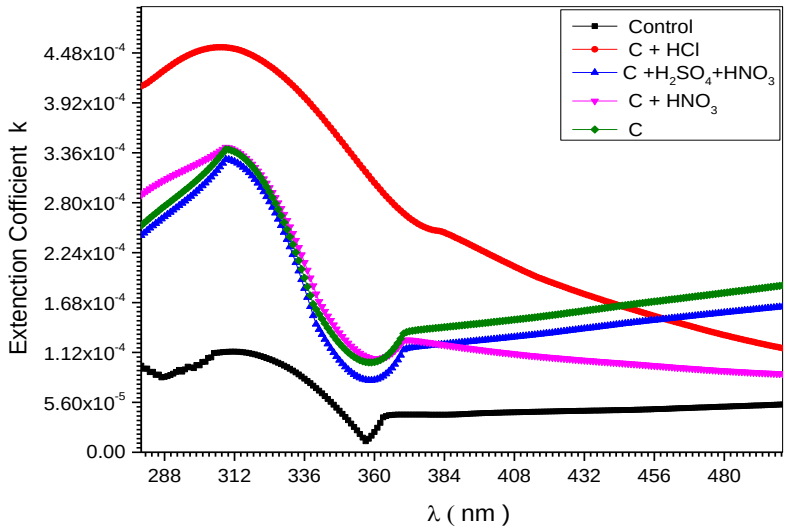

Fig (4.1.5) The Extinction coefficient (K) spectra of Wooden Carbon Sinag treated by three acids (HCL, HNO_3 and H_2SO_4:HNO_3 mixture) and one is untreated compared with control Multi Wall Carbon Nanotube sample (MWCNT).

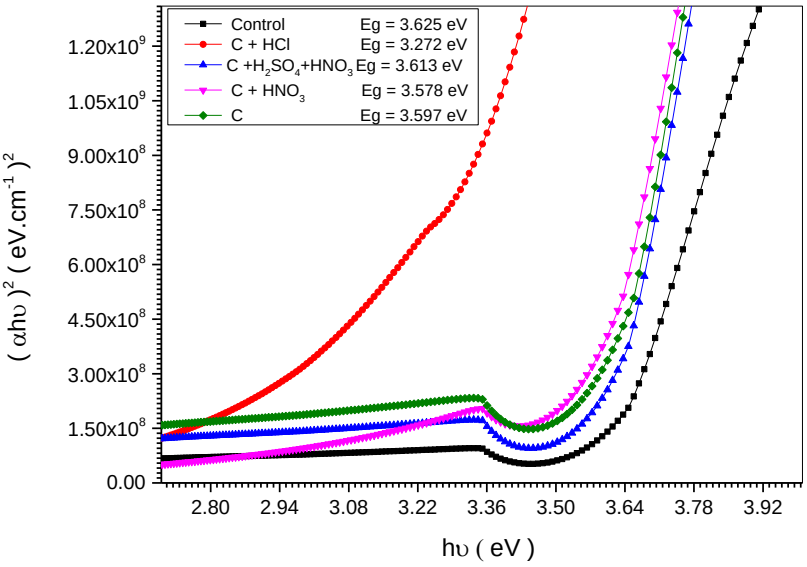

Fig(4.1.6) The optical energy gap (Eg) value of Wooden Carbon Sinag treated by three acids (HCL,HNO_3 and H_2SO_4:HNO_3 mixture) and one is untreated compared with control Multi Wall Carbon Nanotube sample (MWCNT).

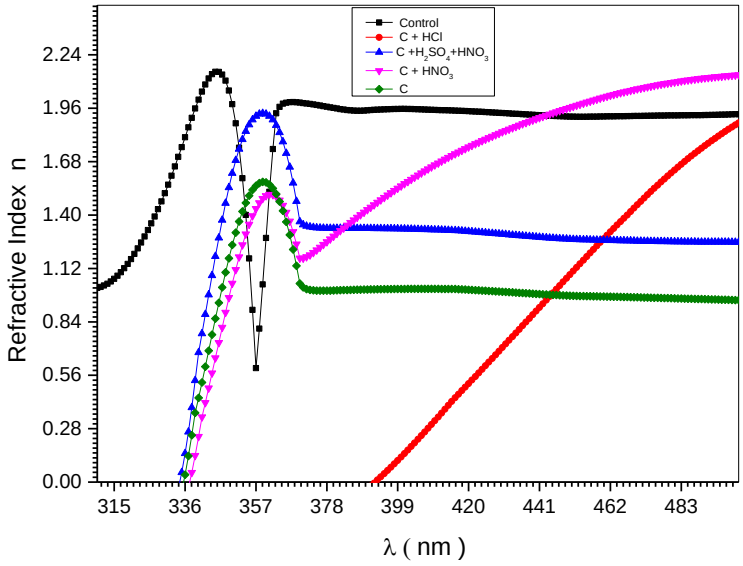

Fig (4.1.7) The refractive index (n) spectra of Wooden Carbon Sinag treated by three acids (HCL,HNO_3 and H_2SO_4:HNO_3 mixture) and one is untreated compared with control Multi Wall Carbon Nanotube sample (MWCNT).

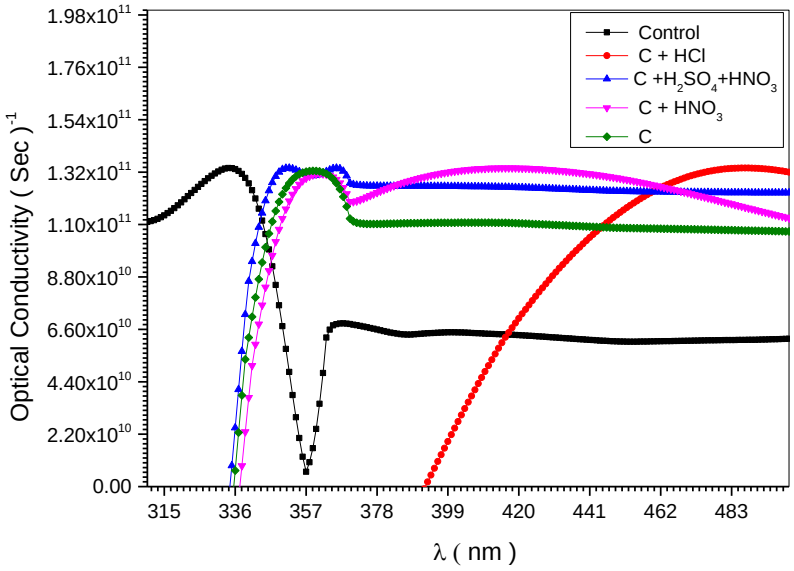

Fig (4.1.8) Plot of optical conductivity spectra of Wooden Carbon Sinag treated by three acids (HCL, HNO_3 and H_2SO_4:HNO_3 mixture) and one is untreated compared with control Multi Wall Carbon Nanotube sample (MWCNT)

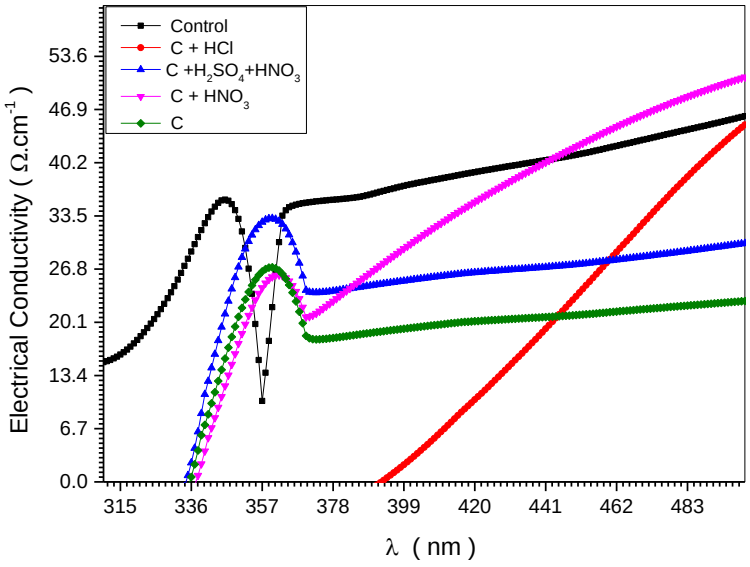

Fig.(4.1.9) Plot of electrical conductivity spectra of Wooden Carbon Sinag treated by three acids (HCL, HNO_3 and H_2SO_4:HNO_3 mixture) and one is untreated compared with control Multi Wall Carbon Nanotube sample (MWCNT)

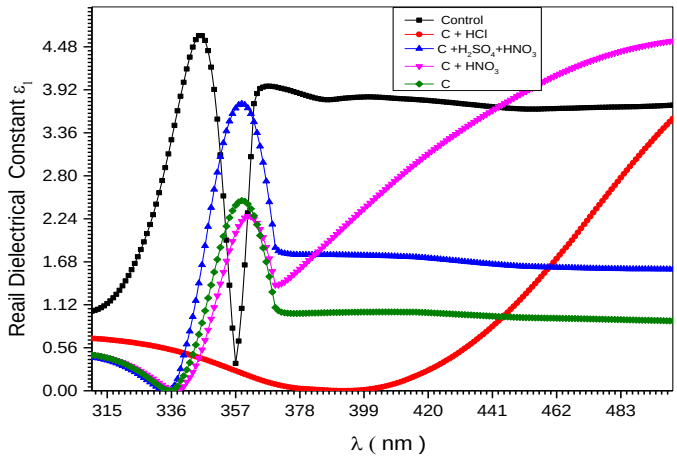

Fig (4.1.10) The real dielectric constant (ε_1) spectra of Wooden Carbon Sinag treated by three acids (HCL, HNO_3 and H_2SO_4:HNO_3 mixture) and one is untreated compared with control Multi Wall Carbon Nanotube sample (MWCNT).

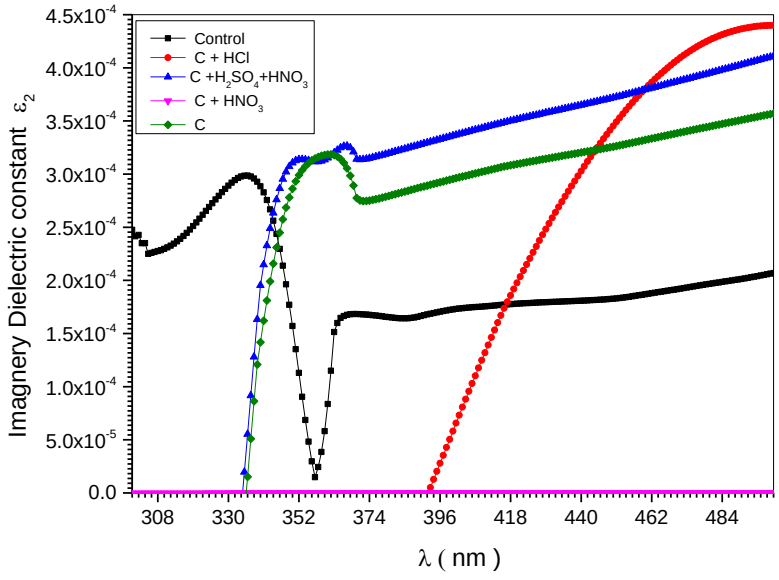

Fig. (4.1.11) The imaginary dielectric constant (ε2) spectra of Wooden Carbon Sinag treated by three acids (HCL,HNO_3 and H_2SO_4:HNO_3 mixture) and one is untreated compared with control Multi Wall Carbon Nanotube sample (MWCNT).

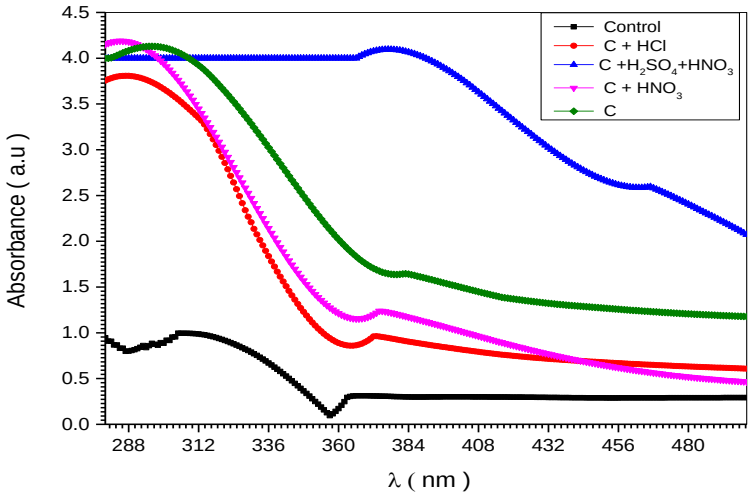

Fig (4.1.12) The optical absorption coefficient spectra of Waste Petroleum Coke Powder (WPCP) treated by three acids (HCL, HNO3 and H_2SO_4:HNO_3 mixture) and one is untreated compared with control Multi Wall Carbon Nanotube sample (MWCNT).

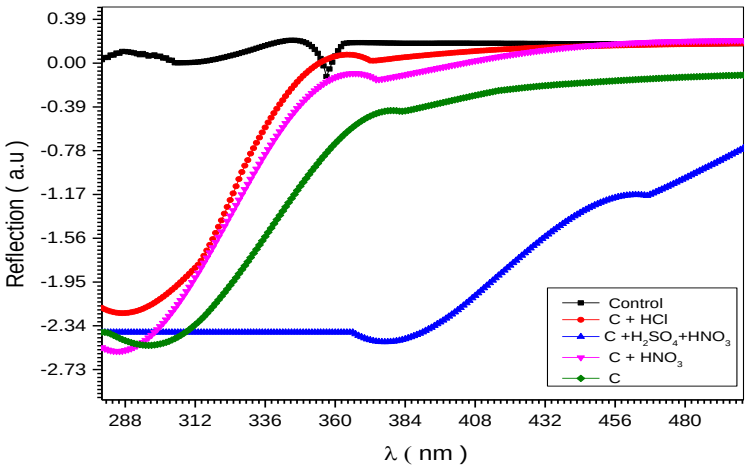

Fig (4.1.13) The optical reflection spectra of Waste Petroleum Coke Powder (WPCP) , treated by three acids (HCL,HNO_3 and H_2SO_4:HNO_3 mixture) and one is untreated compared with control Multi Wall Carbon Nanotube sample (MWCNT).

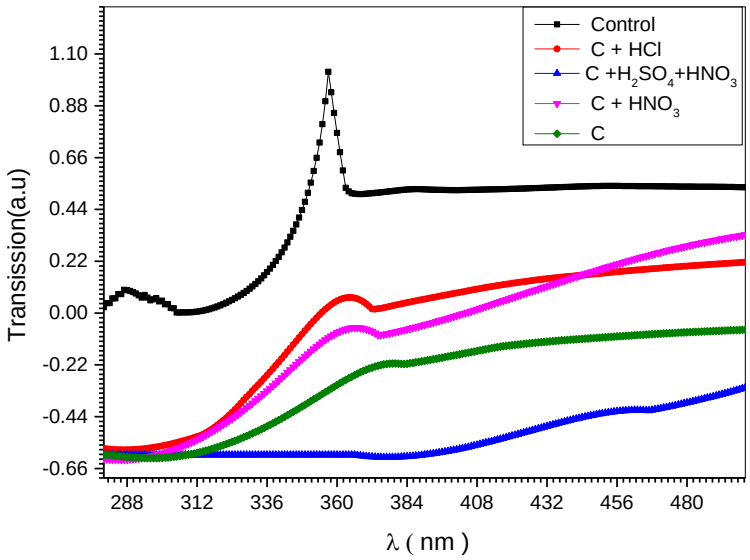

Fig (4.1.14) The optical transmission spectra of Waste Petroleum Coke Powder (WPCP) treated by three acids (HCL, HNO3 and H_2SO_4:HNO_3 mixture) and one is untreated compared with control Multi Wall Carbon Nanotube sample (MWCNT).

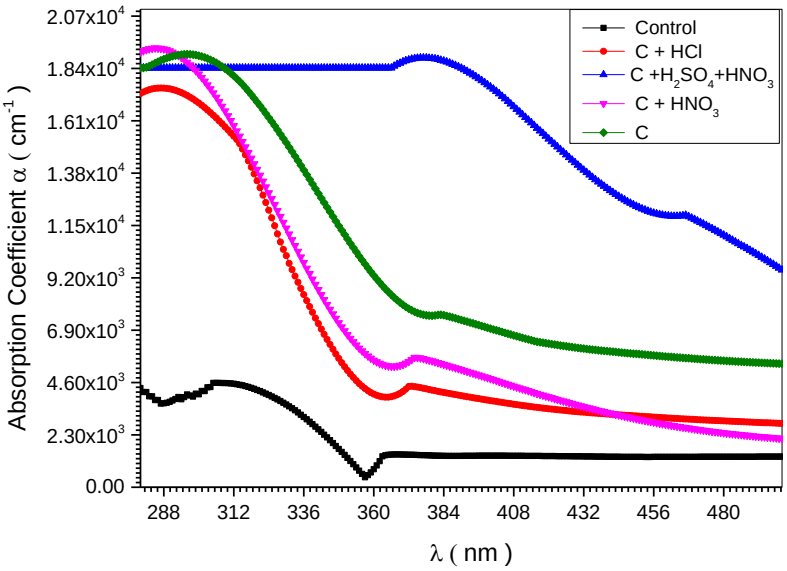

Fig (4.2.15) The optical absorption coefficient spectra of Waste Petroleum Coke Powder (WPCP), treated by three acids (HCL, HNO3 and H_2SO_4:HNO_3 mixture) and one is untreated compared with control Multi Wall Carbon Nanotube sample (MWCNT).

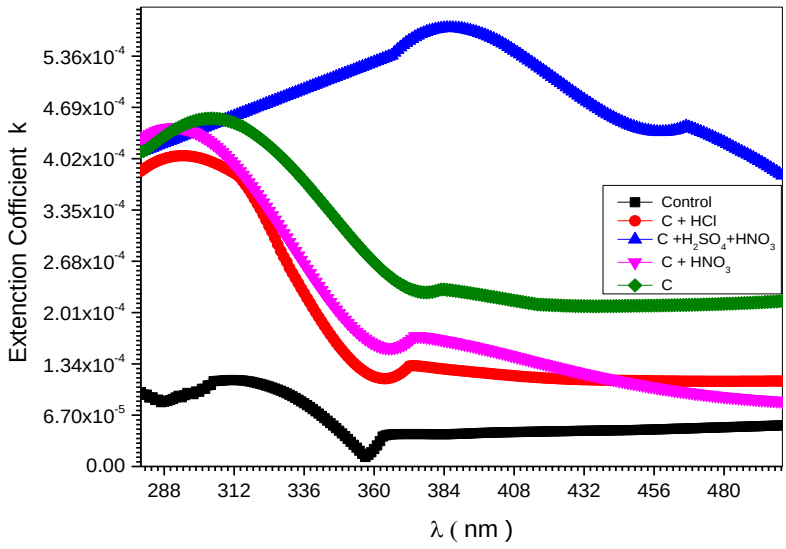

Fig (4.1.16) The Extinction coefficient (K) spectra of Waste Petroleum Coke Powder (WPCP) treated by three acids (HCL,HNO_3 and H_2SO_4:HNO_3 mixture) and one is untreated compared with control Multi Wall Carbon Nanotube sample (MWCNT).

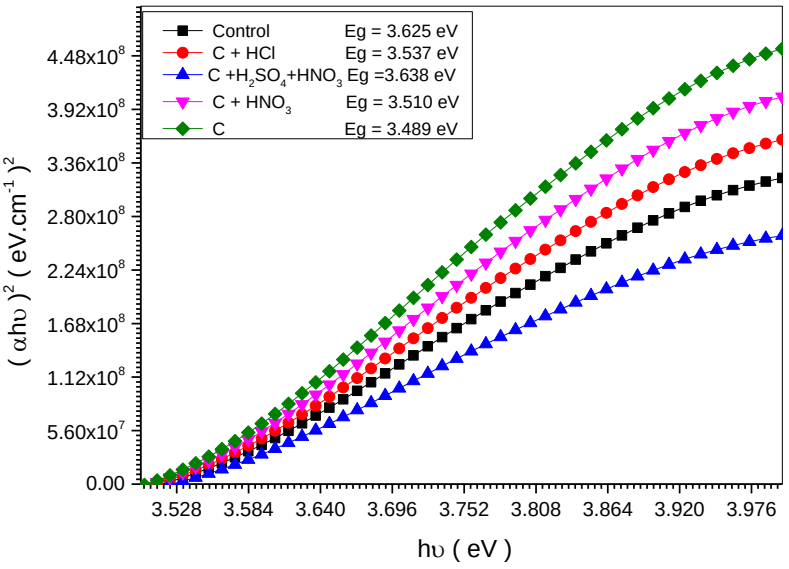

Fig(4.1.17) The optical energy gap (Eg) value of Waste Petroleum Coke Powder (WPCP) , treated by three acids (HCL,HNO_3 and H_2SO_4:HNO_3 mixture) and one is untreated compared with control Multi Wall Carbon Nanotube sample (MWCNT).

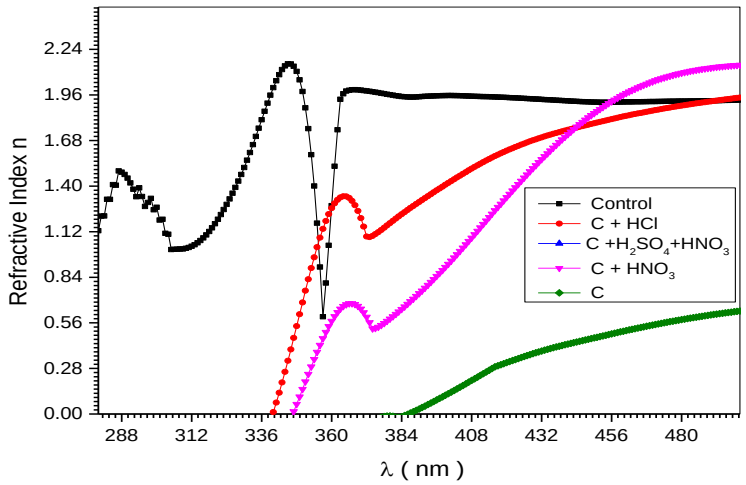

Fig (4.1.18) The refractive index (n) spectra of Waste Petroleum Coke Powder (WPCP) treated by three acids (HCL,HNO_3 and H_2SO_4:HNO_3 mixture) and one is untreated compared with control Multi Wall Carbon Nanotube sample (MWCNT).

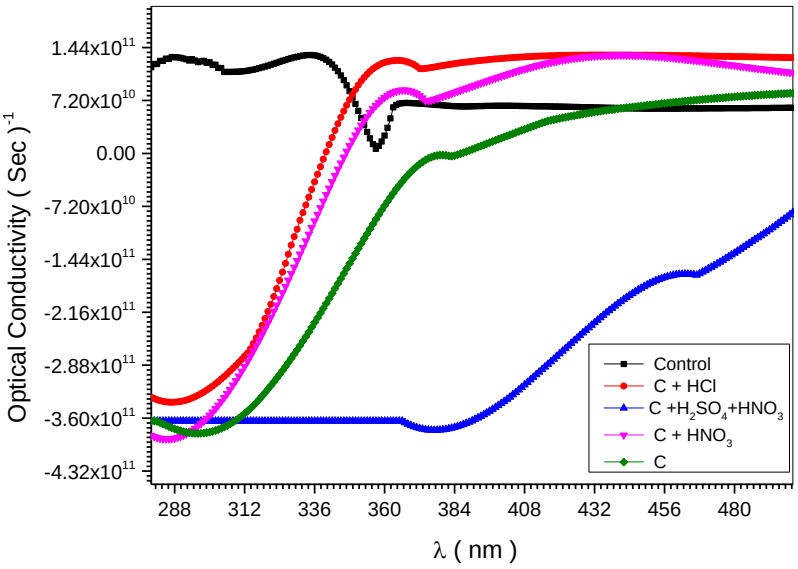

Fig(4.1.19) Plot of optical conductivity spectra of Waste Petroleum Coke Powder (WPCP) , treated by three acids (HCL,HNO_3 and H_2SO_4:HNO_3 mixture) and one is untreated compared with control Multi Wall Carbon Nanotube sample (MWCNT).

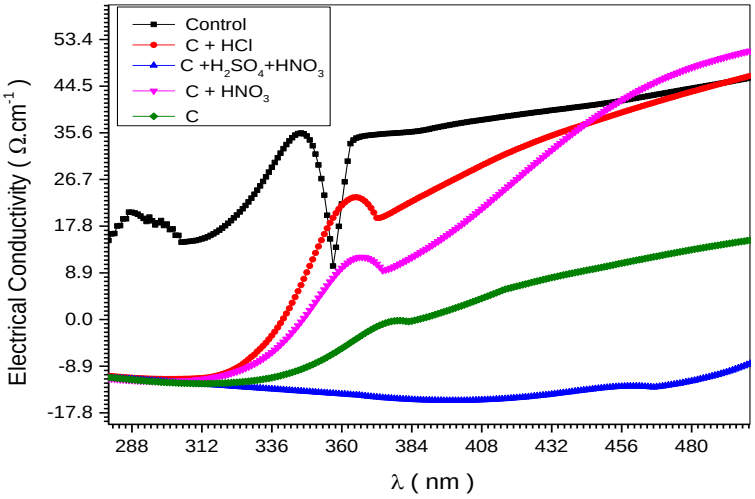

Fig. (4.1.20) Plot of electrical conductivity spectra of Wooden Carbon Sinag treated by three acids (HCL, HNO^3 and H_2SO_4:HNO_3 mixture) and one is untreated compared with control Multi Wall Carbon Nanotube sample (MWCNT).

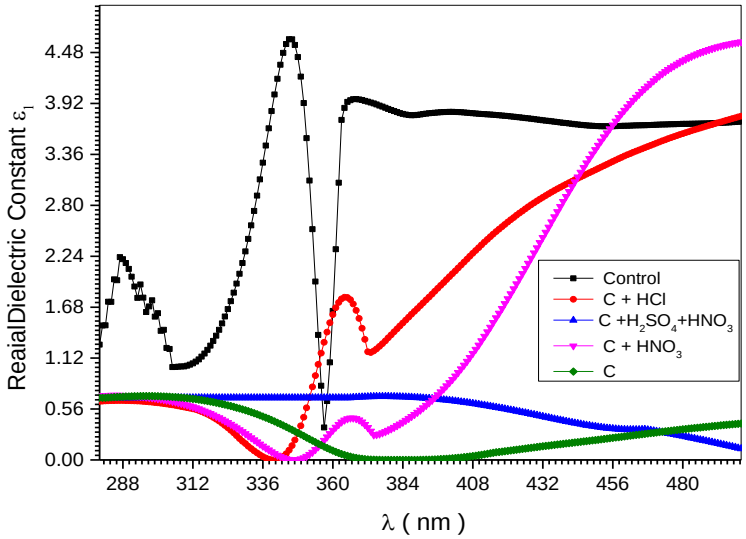

Fig (4.2.21) The real dielectric constant (ε_1) spectra of Waste Petroleum Coke Powder (WPCP), treated by three acids (HCL, HNO3 and H_2SO_4:HNO_3 mixture) and one is untreated compared with control Multi Wall Carbon Nanotube sample (MWCNT).

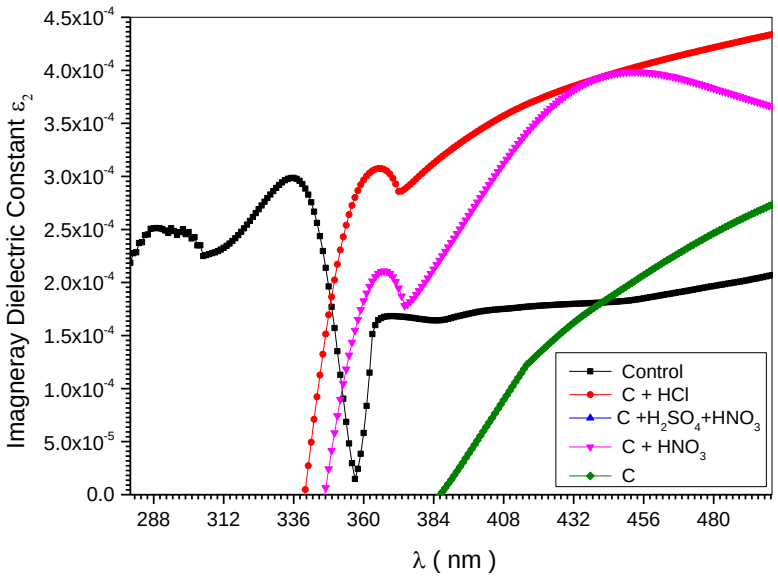

Fig (4,1,22)The Imaginary dielectric constant (ε_1) spectra of Waste Petroleum Coke Powder (WPCP) , treated by three acids (HCL,HNO_3 and H_2SO_4:HNO_3 mixture) and one is untreated compared with control Multi Wall Carbon Nanotube sample (MWCNT).)

4-2 FT-IR Results

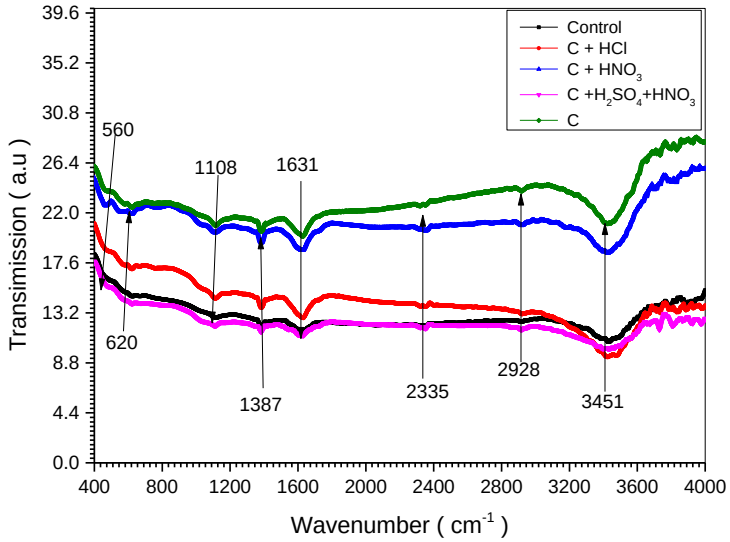

Fig (4.2.1) FTIR spectra of Sinag treated by three acids (HCL,HNO_3 and H_2SO_4:HNO_3 mixture) and one is untreated compared with control Multi Wall Carbon Nanotube sample (MWCNT).

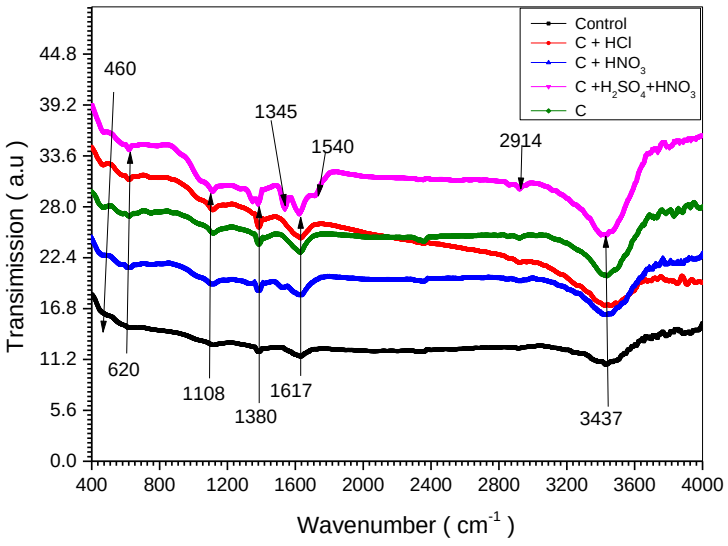

Fig (4.2.2) FTIR spectra of Waste Petroleum Coke Powder (WPCP), treated by three acids (HCL,HNO_3 and H_2SO_4:HNO_3 mixture) and one is untreated compared with control Multi Wall Carbon Nanotube sample (MWCNT).

4.3 Discussion

Absorption coefficient (α) and the extinction coefficient (k) are obtained by relations [9]

$$\alpha = 2.303\ A/t$$

Where (A) is absorbance and (t) is the optical axes length of the sample.

$$K = \lambda\alpha/4\pi$$

Figures (4.1.4) & (4.1.4) shows that the absorption coefficient is large for all samples compared to the control and is maximum for Sinag treated with HCL .The same hold for extinction coefficient. This increase may be due to increase of grain size and decrease of number of defects by heat treatment [9,13].

The optical energy gap (Eg) has been obtained by the relation [11]

$$(\alpha h\upsilon)^2 = C\ (h\upsilon - Eg)$$

Where: (C) is constant, by plotting $(\alpha h\upsilon)^2$ vs photon energy (hυ)

figure (4.1.6) shows that the optical energy gap is less than that of the control for all samples and have minimum value of 3.272 ev for sinag treated with HCL .It is very interesting to note that whenever the absorption coefficient is maximum the energy gap is minimum and vice versa .This agrees with the fact that the relation between energy gap and absorption coefficient is inverse relation. The decrease of energy gap may result from the decrease of density and grain boundaries due to heat treatment [9, 13].

The value of refractive index (n) was obtained from the equation [8]

$$n = [(\frac{(1+R)}{(1-R)})^2 - (1+k^2)\ ]^{\frac{1}{2}} + \frac{(1+R)}{(1-R)}$$

Where (R) is the reflectivity the variation of (n) vs (λ) shown in fig (4.1.7) for all samples is less than that of the control for wave lengths in the range (315-382 nm).The minimum value

is for Sinag treated HCL sample .This conforms with the inverse relation between absorption coefficient and refractive index. The wave length at which (n) is maximum increases from 336 to357 nm. Surprisingly the max for samples coincides with the minimum for the control.

The optical conductivity is a measure of frequency response of material when irradiated with light which is determined using the following relation [11]

$$\delta_{0pt} = \frac{\alpha n c}{4\pi}$$

Where(c) is the light velocity. The electrical conductivity can be estimated using the

Following relation [11].

$$\delta_e = \frac{2\lambda\delta_{0pt}}{\alpha}$$

The optical conductivity in fig (4.1.8) shows maximum value at 357nm for all samples where it is minimum for control .The maximum .value for control is at 336nm.The conductivity for all samples is larger than that of control for all wave lengths larger than 420 nm. Clearly conductivity follows absorption, which conforms to theoretical models.

Absorption coefficient (α) and the extinction coefficient (k) are obtained by relations [9]

$$\alpha = 2.303\ A/t$$

where (A) is absorbance and (t) is the optical axes length .

$$K = \lambda\alpha/4\pi$$

The absorption coefficient in fig (4.1.16) is maximum for (WPCP) treated by H_2SO_4:HNO_3 compared to control and non-treated sample. The other two samples have less value than non-treated one. The increase may be due to increase of grain size and decrease of number of defects by heat treatment [9, 13].

.

The value of refractive index (n) was obtained from the equation [9]

$$n = [(\frac{(1+R)}{(1-R)})^2 - (1+k^2)\,]^{\frac{1}{2}} + \frac{(1+R)}{(1-R)}$$

Where (R) is the reflectivity . The variation of (n) vs (λ) shown in Fig (4.1.18) shows that the refractive index is less than that of the control for all samples at all wave length values less than 485 nm except at about 350 nm , where the control has minimum value at this point. However, for wave lengths more than 485 nm (WPCP) treated by HNO_3 and (WPCP) treated by HCL have larger values compared to control.

The dielectric real and imaginary parts are given by [11]

$$\varepsilon_1 = n^2 - k^2$$

$$\varepsilon_2 = 2nk$$

The real dielectric constant curves, shown in fig (4.1.21), indicates that the dielectric constant is smaller for all samples in the range (288-450 nm) compared to control .However for more than 180 nm (WPCP) treated by $HNO_3$and treated by HCL the values are larger than that of the control .This means that at large wavelengths, where the frequency nearly vanish and the current is nearly direct, the dielectric constant is relatively large. Thus the petrol nano carbon can be used to fabricate nano batteries.

The FTIR optical spectral patterns in figure (4.2.1) and (4.2.2) resembles that of UV except that of the mixture of H_2SO_4:HNO_3 for refractive index where the curve appears to be in arrange less than that exhibited by the graphs.

4.4 Conclusion

The behaviour of locally prepared carbon samples (sinag) shows higher absorption coefficient and conductivity; beside narrower energy gap and smaller refractive index compared to control .The results obtained conform to theoretical relations. The maximum conductivity of petrol samples shifts towards larger wave lengths compared to control. This means that one can maximize conductivity by using less energetic photons. The absorption coefficient is maximum when treated with both H_2SO_4&HNO_3.The refractive index and the real dielectric constant, are however smaller for smaller wave lengths ,while the ones treated with HNO_3&HCL have larger values for larger wave lengths. The FTIR technique results confirm that obtained by UV.

4.5 Recommendation

1-The locally prepared powders of carbons can be utilized in storing electric energy and fabrication of integrated nano conductor.

2-The properties of these carbon powders can be improved by using other solvents.

3-Thermal properties of these carbon powders can be also investigated.

4-The carbon powders prepared from different treats can be compared with each other to study the effect of chemical composition and physical structure.

4.6 References

[1] Jan Prasek, Methods for carbon nanotubes synthesis—review, The Royal Society of Chemistry (2011) 15872–15884.

[2] Ernesto Joselevich, Carbon Nanotube Synthesis and Organization, A. Jorio, G. Dresselhaus, M. S. Dresselhaus (Eds.): Carbon Nanotubes,Topics Appl. Physics(2008) 111, 101–164 .

[3] E.R. Edward-Evaluation of residual iron in carbon nanotubes purified by acid treatments/ Applied Surface Science 258 (2011) 641– 648.

[4] Muhammad Ali Turgunov1, Surface Modification of Multiwall Carbon Nanotubes by Sulfuric Acid and Nitric Acid , Advanced Science and Technology Letters Vol.64 (Materials 2014) . pp.22-25 .

[5] M. STANCU, Purification of multiwall carbon nanotubes obtained byAC arc discharge method , OPTOELECTRONICS AND ADVANCED MATERIALS – RAPID COMMUNICATIONS , Vol. 5, No. 8, August 2011, p. 846 – 850 .,

[6] M. Vesali Naseh , Functionalization of Carbon Nanotubes Using Nitric Acid Oxidation and DBD Plasma , World Academy of Science, Engineering and Technology 49 2009 .

[7] V. Datsyuk, M. Kalyva , Chemical oxidation of multiwalled carbon nanotubes , Elsevier , science direct C A R B ON 46 (2008) 8 33 –840 .

[8] Fu-Hsiang Ko , Chung-Yang Lee , Chu-Jung Ko , Purification of multi-walled carbon nanotubes through microwave heating of nitric acid in a closed vessel , Elsevier science direct Carbon 43 (2005) 727–733 .

[9] Kevin A. Wepasnick a, Billy A. Smith , Surface and structural characterization of multi-walled carbon nanotubes following different oxidative treatments , Elsevier science direct , CARBON 4 9 (2011) 24 –36 .

[8] Mohammed Fadhil AL-Mudhaffer, Optical Parameters and Absorption Studies of Benzene-sulfonamide Azo Dye Thin Film Prepared by Spray Pyrolysis Method , Department of Physics, College of Education, University of Basrah, Basrah, Iraq .

[9] Hamid S. AL-Jumaili , Effect of thermal annealing and laser radiation on the optical properties of AgAlS2 thin films , Iraqi Journal of Physics , 2011, Vol. 9, No.16, PP. 79-83.

[10] F.I. Ezema , A.B.C. Ekwealor and R.U. Osuji :Turk.J.Phys.30, (2006) pp.1-7.

[11] S. Wang and H. Li , Dyes Pigm ,72, 308-314. (2007) .

[12] H. Idriss , Effect of Acetylene Rates and Temperature Variations of Iron and Cobalt Nanoparticles in Carbon Nanotubes Fabrication ,1 Physics Department, College of Science, Sudan University of Science technology, Khartoum 11113, Sudan, April 2017 .
[13]F.I. Ezema , A.B.C. Ekwealor and R.U. Osuji :Turk.J.Phys.30, (2006) pp.1-7.Sudan University of Science technology, Khartoum 11113, Sudan, April 2017
[14] Rotem Marom , Enhanced performance of starter lighting ignition type lead-acid batteries with carbon nanotubes as an additive to the active mass, Journal of Power Sources 296 (2015) 78e85
[15] Agathe Figarol , In vitro toxicity of carbon nanotubes, nano-graphite and carbon black, similar impacts of acid functionalization , Published by Elsevier B.V 2015
[16] Huo Q, Margolese D I and Stucky G D 1995 Science 267 865 0887-233

[17] C. Denktas , Effect of multi wall carbon nanotube on electrical properties 4-[4-((S)-Citronellyloxy)benzoyloxy]benzoic acid liquid crystal host, Elsevier Ltd. All rights reserved, 2015 1359-8368.
[18] Lampart C.M. and Granquist C.G.1990: SPIE, Optical Engineering Press, Bellingham WA.
[19] Antonelli D M and Ying J Y 1995 Angew. Chem., Intl. Ed. Engl. 34 2014.
[20] Sangho Chung , Enhanced electrical and mass transfer characteristics of acid-treated carbon nanotubes for capacitive deionization, Current Applied Physics 15 (2015) 1539e1544
[21] Pulickel M. Ajayan and Otto Z. Zhou. Applications of Carbon Nanotubes. Chem. (2016), 17.pp. 393-425.
[22]Allemann E., Gurny R., Doekler E. Drug-loaded nanoparticlespreparation methods and drug targeting issues. Eur J Pharm Biopharm. 1993; 39:173-91.
[23] Betancor L. and Luckarift HR. 2008 Trends Biotechnol. 26 566 Dunne M, Corrigan Bodmeier R., Chen H. Indomethacin polymeric nanosuspensions prepared by micro-fluidization. J Control Release. 1990; 12:223-33.
[24] Catarina PR., Ronald JN., Antonio JR. Nano capsulation 1. Method of preparation of drug – loaded polymeric nanoparticles: Nano technology, Biology and medicine. 2006; 2:8-21.